Imaging through thick turbid medium using time-resolved measurement

Guy Satat, Dan Raviv, Barmak Heshmat, Ramesh Raskar

Media Lab, Massachusetts Institute of Technology, 77 Massachusetts Ave., 02139, Cambridge, MA, USA

guysatat@mit.edu

Abstract: We propose and experimentally demonstrate a novel method to image a scene hidden behind a 1.5cm thick scattering medium. Our method is based on time-resolved measurement combined with an optimization framework for inversion.

OCIS codes: (110.0113) Imaging through turbid media, (290.0290) Scattering.

1. Introduction

Imaging through scattering media is a long lasting problem in optics, as standard direct imaging techniques fail due to scattering. Different modalities to overcome scattering utilize various properties of light, such as coherence (e.g. optical coherence tomography [1]), time-reversal (e.g. phase-conjugate methods such as [2]) and ballistic photons [3]. In this work we use time-resolved measurement which is based on the finite speed of light. Using time-resolved measurement to overcome scattering through a thin layer was previously demonstrated in [4]. In this work we use it for measuring the imaging system point spread function (PSF) in space as well as in time, which enables reconstructing a scene hidden behind volumetric scattering. We demonstrate a reconstruction of a mask hidden behind a 1.5cm thick tissue phantom. Our method uses all photons for imaging (ballistic, diffused, coherent, etc.); thus it has improved signal-to-noise characteristics compared to other techniques that use only part of the photons.

2. Methods

Fig. 1 shows schematic and photographs of our optical setup. A Ti-Sapph laser (795nm, 75MHz repetition rate and 50fs pulse duration) is focused onto a polycarbonate diffuser. The diffused light illuminates a mask which is stacked on the back of a thick tissue phantom (1.5cm thick silicon-based phantom). A streak camera (with time resolution of 2ps and 1ns acquisition window) is focused onto the front side of the tissue phantom through a set of rotating mirrors. The mirrors are used to scan through the y-dimension of the system with periscope-like mechanism (this is required because the streak tube is imaging just a single line in the y-dimension). For each position of the rotating mirrors a streak image is captured. The result is a complete measurement of the $x-y-t$ space.

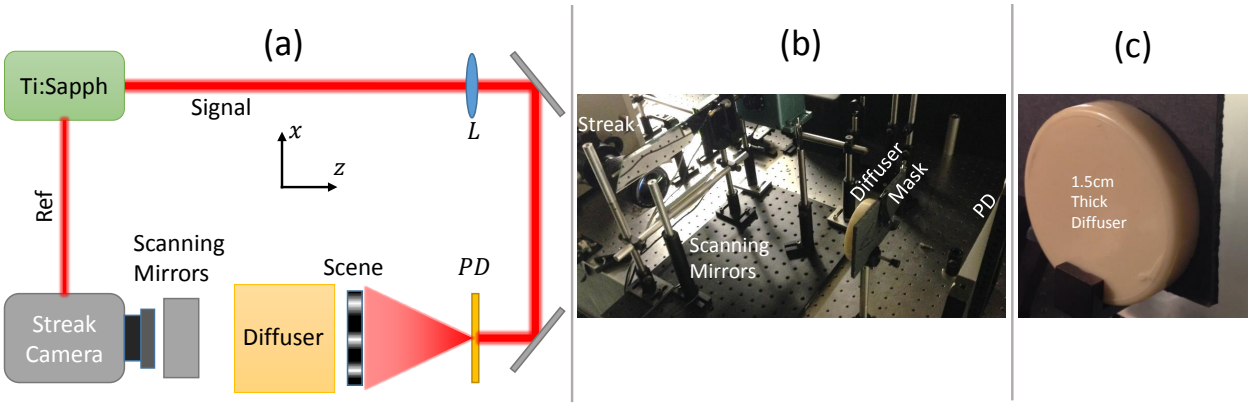

Fig. 1. (a) Optical system setup. L is a lens focusing the laser beam on a polycarbonate diffuser (PD). (b) Experimental setup. (c) Photograph of the thick tissue phantom with a mask hidden behind it.

We characterize the system PSF by placing a pin-hole mask behind the phantom. Fig. 2a shows the measurement cross section for $y = 0$. The scattering blurs the signal in both spatial and time axis. First we analyze the time response. Fig. 2b shows the average time response which demonstrates a quick rise and slow decay. We empirically fit this time response with a log-normal curve:

$$f_T(t) = \frac{1}{t} e^{-\frac{(\ln t - \mu)^2}{2\sigma^2}} \tag{1}$$

where μ and σ are fitted empirically. After normalizing with the time response (Fig. 2c) we get a classical time-dependent diffusion which is characterized by:

$$f_S(x,y,t) = e^{-\frac{x^2+y^2}{4(D_0+D_1 t)}} \tag{2}$$

where D_0 and D_1 are fitted empirically. Combining equations 1 and 2 we get the system space-time PSF:

$$PSF(x,y,t) = \frac{1}{t} e^{-\frac{(\ln t - \mu)^2}{2\sigma^2}} e^{-\frac{x^2+y^2}{4(D_0+D_1 t)}} \tag{3}$$

Fig. 2d shows the result of plotting Eq. 3 for $y = 0$.

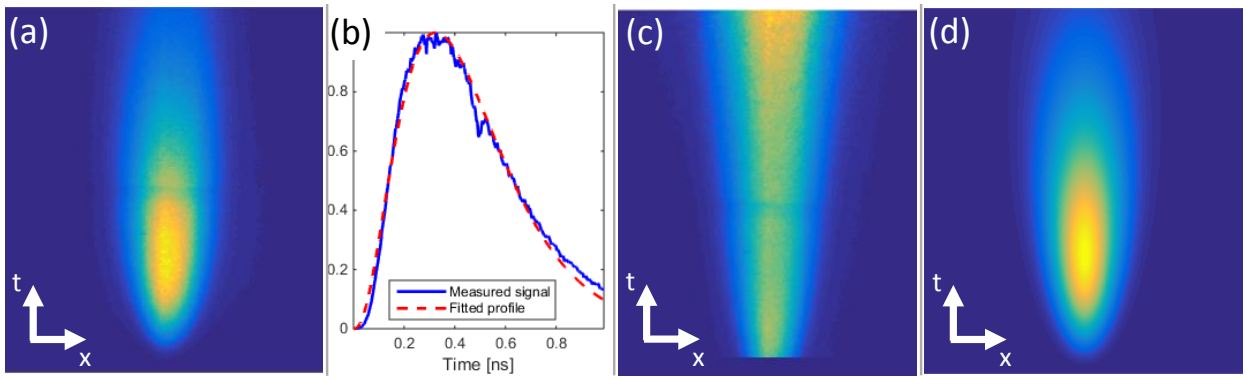

Fig. 2. Fitting an analytical expression for the system PSF. (a) Measurement of the system PSF, a cross section of the $x-t$ plane for $y = 0$. (b) Average of time response (blue) and fitted curve according to Eq. 1. This fit results in a coefficient of determination $R^2 = 0.995$ (c) The result of normalizing the measured PSF (Fig. 2a) with the time profile in Eq. 1. (d) Cross section of Eq. 3 of the $x-t$ plane for $y = 0$ (compare to Fig. 2a).

To summarize, our model has 4 parameters which can be easily fitted. Fig 2b demonstrates fitting μ, σ and Fig. 2c demonstrates fitting D_0, D_1. We note that this PSF is a result of a point source at the center of the mask plane $(x',y') = (0,0)$ and for a pulse hitting the mask at $t = 0$. Thus, for a point source at position (x',y') our measurement will be:

$$M(x,y,t,x',y') = \frac{1}{t} e^{-\frac{(\ln t - \mu)^2}{2\sigma^2}} e^{-\frac{(x-x')^2+(y-y')^2}{4(D_0+D_1 t)}} \tag{4}$$

We discretize the mask plane, and using Eq. 4 generate a synthetic measurement for each discreet position (x',y'). Each three dimensional measurement tensor M is vectorized (we define a vectorizing operator $V : \mathbb{R}^3 \to \mathbb{R}$ which simply rearranges the tensor entries into a vector). We stack the measurement vectors of different positions in a matrix A, such that each column corresponds to a vectorized measurement $V(M)$ of a single point source in a specific (x',y') position.

We denote an actual measurement of our imaging system as b (i.e. the full $x-y-t$ space), and our goal is to recover a vector $\hat{s}$ such that

$$V(b) = A\hat{s} \tag{5}$$

where different entries in $\hat{s}$ correspond to different (x',y') locations on the hidden 2D mask. The problem in Eq. 5 is still ill-posed since A is non-invertible. To make the problem better-posed we add a regularizing term which assumes

a piece-wise smooth scene:

$$\hat{s} = \arg min_s \|As - V(b)\|_2^2 + \lambda \|s\|_1 \quad (6)$$

where we use the $\ell 1$ norm ($\|s\|_1 = \sum_i |s_i|$). Adding an $\ell 1$ regularizer is common for promoting sparsity (as opposed to the $\ell 2$ norm which promote smooth reconstruction). To solve the problem in Eq. 6 we use a combination of gradient descent and proximal operator for soft thresholding similar to those described in [5]. The final hidden scene is finally recovered by rearranging the entries in the vector $\hat{s}$ to the corresponding (x', y') positions.

3. Results

Finally, to demonstrate our technique in reconstructing a two-dimensional scene, we place a mask (Fig. 3a) behind the thick diffuser. Fig. 3b shows the result of averaging the measurement along the time axis (serving as a baseline for comparison to a non-time-resolved measurement). The result of the suggested reconstruction process is demonstrated in Fig. 3c. This result can be thresholded to get a better binary result as seen in Fig. 3d. As can be seen from this demonstration, our method successfully recovers the hidden scene features.

We note that the relatively low reconstruction resolution is due to computational and not physical constraints. In order to reduce computational burden, we significantly discretize the mask plane (such that the matrix A fits in memory). Using a stronger computer or a more efficient algorithm would enable higher resolution reconstructions.

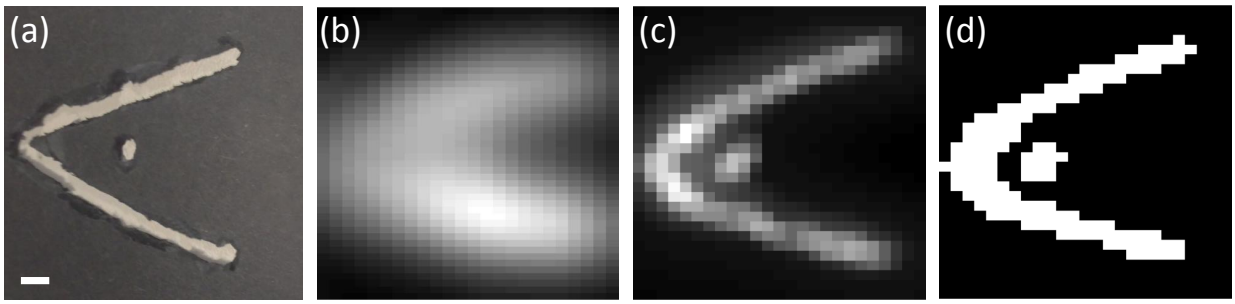

Fig. 3. Successful experimental reconstruction of a hidden scene. (a) The mask hidden behind the diffuser (white scale bar: 4mm). (b) Imaging without using time-domain information. (c) Reconstruction using the suggested algorithm. (d) Applying a threshold to generate a binary image from the reconstruction in panel (c).

4. Conclusions

We demonstrate a method to recover a scene hidden behind thick scattering medium. Our method uses time-resolved measurement to increase the dimensionality of the problem, thus making it better-posed. Comparing the suggested reconstruction technique to a non-time-resolved one shows that measuring time profile significantly improves the stability of the algorithm and allows to recover the mask features. Furthermore, the technique does not depend on specific characteristics of photons such as coherence, ballistic, etc.; all photons are used, which results in improved signal-to-noise performance. Our approach has potential applications in remote sensing and bio-medical imaging.

References

1. D Huang, EA Swanson, CP Lin, JS Schuman, WG Stinson, W Chang, MR Hee, T Flotte, K Gregory, CA Puliafito, and al. et. Optical coherence tomography. *Science*, 254(5035):1178–1181, 1991.
2. I M Vellekoop, A Lagendijk, and A P Mosk. Exploiting disorder for perfect focusing. *Nat. Photonics*, 4(5):320–322, 2010.
3. L Wang, P P Ho, C Liu, G Zhang, and R R Alfano. Ballistic 2-d imaging through scattering walls using an ultrafast optical kerr gate. *Science (New York, N.Y.)*, 253(5021):769–71, 1991.
4. G Satat, B Heshmat, C Barsi, D Raviv, O Chen, M Bawendi, and R Raskar. Locating and classifying fluorescent tags behind turbid layers using time-resolved inversion. *[under review]*, 2015.
5. P Combettes and V Wajs. Signal Recovery by Proximal Forward-Backward Splitting. *Multiscale Modeling & Simulation*, 4(4):1168–1200, 2005.